Analysis Of Backscatter To Extraction Of Shoreline Using Machine Learning Methods In The Bangkalan Regency

Fahmi Arifin[1], *Ashari* Wicaksono[1,2*]

[1] Department of Marine Science, University of Trunojoyo Madura, Jl. Raya Telang PO BOX 2 Kamal-Bangkalan, East Java, Indonesia
[2] Laboratory of Oceanography, University of Trunojoyo Madura, Jl. Raya Telang PO BOX 2 Kamal-Bangkalan, East Java, Indonesia

Abstrak. Coastal areas are often threatened by natural and anthropogenic factors, causing instability and shoreline changes in the affected areas. Shoreline changes can be monitored with remote sensing techniques such as Synthetic Aperture Radar (SAR) data. The purpose of this research is to extract the coastline by segmenting the machine learning method and find out how far the machine learning model works to distinguish the water class and the land class. The method used in this research is the Support Vector Machine model to divide the water and land classes that will be utilized to obtain shoreline extracts from the model results, and evaluate the model by calculating the model accuracy. The overall accuracy results recorded in 2016 and 2023 are 99.5% and 99%, respectively, with Kappa Coefficients of 0.99018 and 0.98138. This study highlights the potential of SAR data and SVM methods in monitoring coastal dynamics and can serve as a reference for sustainable coastal management.

1. Introduction

Coastal areas play an important role in supporting biodiversity and human activities, which also affect the economic development of the surrounding area [1]. Coastal areas are often threatened by natural and anthropogenic factors, causing instability and shoreline changes in the affected areas [2]. Shorelines can be affected by natural activities, such as tides, erosion, sedimentation and sea level rise, which require accurate monitoring to reduce negative impacts [3]. The coastline in Bangkalan Regency has experienced significant changes in recent years. This can occur due to natural processes and human activities, that are quite often carried out in coastal areas [20].

Shoreline changes can be monitored with remote sensing techniques, such as Synthetic Aperture Radar (SAR) data [4]. SAR is a radar system that records the earth's surface through electromagnetic wave signals [10]. SAR is an active sensor that emits energy radiation to get reflections from the object [5]. SAR has advantages over other optical images because it is not affected by clouds, weather, or time (day and night). These advantages can be utilized to

*Corresponding author: ashari.wicaksono@trunojoyo.ac.id

extract the coastline without worrying about problems in other optical images [6]. SAR, especially Sentinel-1, has a high spatial resolution of up to 10 meters, which is good enough to be used for coastline extraction. Sentinel-1 has a wide global coverage with a period of 6-12 days [7]. The frequency emitted by Sentinel-1 is around 5.405GHz, with a wavelength of 5.5 cm [8].

The use of SAR data can be utilized as coastline monitoring by extracting the coastline using several methods. The method that can be used is machine learning, one of which is the Support Vector Machine (SVM) method [9]. The utilization of this SVM method has been carried out in many studies, one of which is to identify Land Cover in an image. This research will utilize SVM to extract coastlines by separating SAR data from two different classes, for example water areas and land areas [9]. The purpose of this research is to extract the coastline by segmenting it using a machine learning method and to determine how well the machine learnig model works to distiguwish the water class from the land class. This research is expected to be a reference for future research that wants to utilize machine learning for coastal dynamics analysis.

1 2. Materials and Method

2.1 Research Location

The research site I selected concentrated on the seaside region of Bangkalan Regency (**Figure 1**). Bangkalan Regency possesses a substantial coastal expanse hence, it was chosen for coastline extraction. At the research site, I partitioned the area into five segments to align with the coastline's outlines, so facilitating the identification of significant variations in abrasion and accretion [11, 12, 13]. Each segment has a different size, as it relates to the dominance of abrasion or accretion occuring in the area [14, 15].

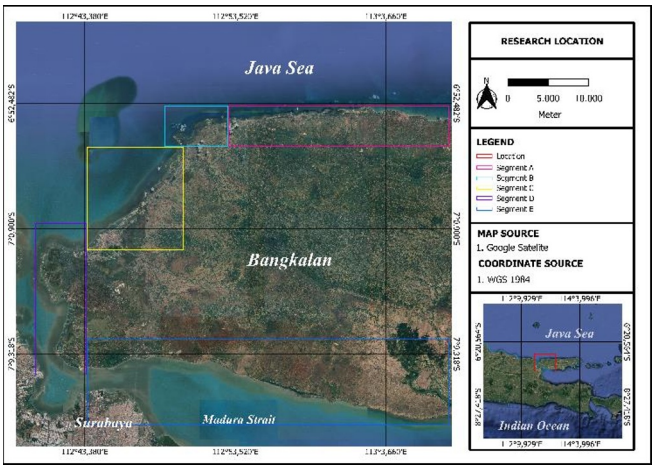

Figure 1. Map of the study area at Bangkalan Regency

2.2 Data Collection

This study uses Sentinel-1 SAR data from November 2016 and November 2023 (Table 1). The SAR data we used was obtained from *https://search.afs.alaska.edu/*. SAR data was selected because its high spatial resolution enhances the accuracy of extracted coastlines. The

Sentinel-1 product used is GRDH with IW recording mode and has VV+VH polarization, but we only use VH polarization. The resolution on the GRDH product is 20 meters which is sufficient to extract the coastline using satellite imagery [8].

Table 1. Sentinel-1 image data used in the research

Date Acquired	Satellite	Product	Acquisition Mode	Polarization	Spatial Resolution
11/11/2016	**Sentinel-1**	GRDH	IW	VH	20 m
11/15/2023	**Sentinel-1**	GRDH	IW	VH	20 m

2.3 Methods

2.3.1 Pre-processing SAR image

Pre-processing is done to improve the quality of the image data before further analysis. This stage is important because the Sentinel-1 image in the GRDH product still contains some noise that can affect the analysis results [17]. The pre-processing steps we conducted included several stages starting from Apply orbit files, Thermal Noise Removal, Remove-GRD Border Noise, Radiometric Calibration, Speckle Filter, Terrain Correction, and Convert Linear to/form dB (Figure 2). After pre-processing, the image subset is carried out to take the desired area precisely in Bangkalan Regency [16].

Pre-processing is done with the help of the ESA SNAP software, which can be obtained for free. The most important pre-processing is in Radiometric correction, which serves to improve the accuracy of the recorded backscatter intensity values [38]. Sigma band output was selected for this radiometric correction process. The next process is the Speckle filter which serves to reduce noise but still retain the important details of the image using the Lee Sigma filter on the image used [39]. Next, Terrain Correction is one of the important steps performed in pre-processing and serves to remove geometric distortions in the image [40]. Terrain correction also improves geolocation accuracy where each pixel produced by the image has the correct coordinates [41]. Terrain correction corrects these distortions with the help of a Digital Elevation Model (DEM) [42]. Pre-processing is the most important thing to do in processing image data.

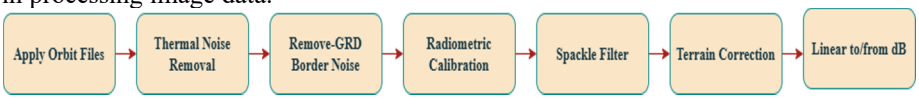

Figure 2. Backscatter before pre-processing and after pre-processing 2016 and 2023

2.3.2 Support Vector Machine

Support Vector machine is a type of supervised learning algorithm used to solve regression and classification problems [18]. SVM can effectively classify data that has a linear or non-linear distribution with the help of a hyperplane. The hyperplane itself is a line that can clearly separate two classes in a dimension. Data points or vectors that are near the hyperplane are called support vectors. Support vector has a role to separate two classes with a high margin. Margin is the distance between two hyperplanes that separate classes from each other in a data. The use of SVM in linear classification can accurately classify two classes, but in image data that has a non-linear function, the classification of the two classes will get poor results [19]. SVM can also classify in the form of non-linear data by using kernel tricks. There are several kernels in non-linear SVM classification, one of which is the Radial Basis Function

(RBF) technique. This research uses RBF as a kernel in SVM classification because this kernel is quite popular and has good performance from other kernels [19].

Other kernel types such as Linear kernel are used for linearly separable data, but for surface data that is non-linear in nature, the linear kernel is not effective [35]. Polynomial kernel is suitable for non-linear data, but often requires many parameters that cause overfitting [36]. The use of RBF kernel is suitable for separating land and water segments using SVM [19]. In addition, the use of the RBF kernel is also commonly used to segment land and water, diubah menjadi "simplifying the process of achieving the desired results [37]. Studies comparing kernel performances show that the RBF kernel achieves the highest accuracy [35]. For example, the linear kernel achieves an accuracy of 86.63%, the polynomial kernel reaches 88.67%, and the RBF kernel achieves the highest accuracy at 90.63% [35].

2.3.3 Accuracy

Model evaluation in machine learning is very much needed, this is because evaluation aims to measure how well the model works with the data that has been given [21]. Model evaluation has various types, such as examples are overall accuracy and kappa coefficient. Both evaluation methods can test the classification model of the model used. Overall Accuracy (OA) measures the percentage of correct predictions across all data. It provides an overview of the model's performance [22].

$$Overall\ Accuracy\ (OA) = \left(\frac{Number\ of\ data\ classified\ correct}{Total\ of\ number\ data}\right) \times 100 \quad (1)$$

Kappa coefficient (K) is used to provide a more in-depth evaluation. Kappa coefficient measures the agreement between model predictions and actual labels by calculating the probability of random agreement [23].

$$Kappa\ Coefficient\ (K) = \left(\frac{Observed\ agreement - Expected\ agreement}{1 - Expected\ agreement}\right) \times 100 \quad (2)$$

3 Result and Discussion

3.1 Backscatter Analysis

Backscatter analysis is performed to understand the radar reflectivity characteristics of land and water surfaces [24]. Backscatter is one of the key parameters in radar data analysis as it provides real-time information about the condition of the scanned surface [25]. This research analyzes the backscatter value to see and identify the study area in 2016 and 2023. Backscatter analysis on image data that has been done and has not been pre-processed has different backscatter values. Backscatter values before pre-processing are usually still in the form of amplitudes that are difficult to interpret directly on the data [26]. The initial backscatter value is usually not calibrated so that there is still a lot of distortion or noise in the data so that the analysis will not run smoothly. Noise in the image data is caused by coherent interference between signals reflected from different surfaces [27]. Noise also makes the real value in the image look random so that pre-processing treatment is needed in the analysis of a SAR image to remove noise by radiometric correction and Speckle Filter [28].

In addition to the noise in the data, the raw image data has also not adjusted to the appropriate coordinate points, so it is very necessary to do one of the pre-processing [29]. Image data that has been geometrically corrected will return to the actual coordinates [29].

The pre-processing carried out has its own role to maximize the data for the following analysis. The next pre-processing step is to change the amplitude value which is the raw signal value from the radar to sigma0 which is the backscatter value that has been done radiometric calibration, then change the sigma0 value into intensity with a decibel (dB) value [16]. The process of changing the value is very important for further analysis because it is easier to interpret the value of data.

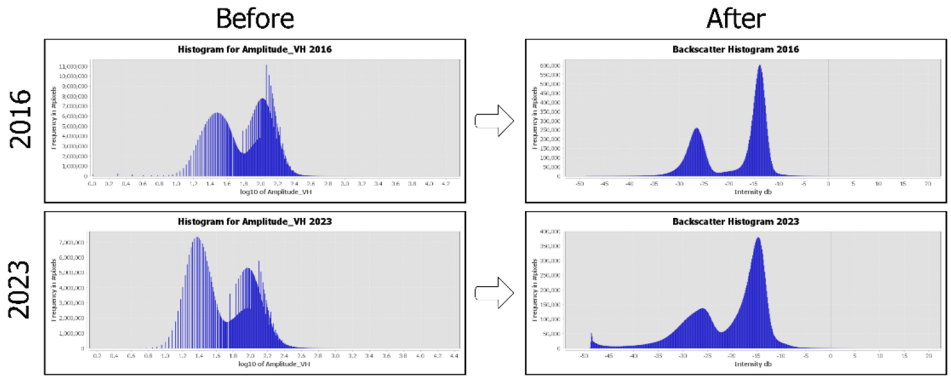

Figure 3. Backscatter before pre-processing and after pre-processing 2016 and 2023

Figure 3 shows a comparison of histograms before and after pre-processing. As previously explained, the value of each pixel in the image data that has not been pre-processed, the value of the data has a value ranging from 0 to 4.4 but there are 2 peaks in the distribution, namely with a value of 1.2-1.4 while the other peak has a value of 2.0-2.4, the value of the two peaks in 2016 and 2023 looks almost uniform. In contrast to the data that has been pre-processed where the backscatter value has been converted in decibel (dB) units, the bacscatter intensity values range from -50dB to 20dB. The value distribution becomes easier to interpret because it has a wider range of values compared to image data that has not been pre-processed. The distribution of values in the image after pre-processing where the first peak has a value range of -30dB to -25dB and the second peak ranges from -15dB to -10dB. The first peak is a low backscatter value that has a class like water area and the second peak shows a high backscatter class that identifies land [30].

The backscatter value on a smooth water surface tends to be lower because the surface is relatively smooth with respect to wavelength, so most of the energy is reflected specularly and away from the sensor [43]. Backscatter values on rougher water surfaces tend to have slightly higher values [43]. Backscatter values on land surfaces are higher due to roughness and heterogeneity in wavelength [44]. Urban areas, vegetation and soil type provide variations in backscatter values [45]. Areas of dense vegetation and tall buildings have relatively higher values than vacant land which has intermediate values [45]. This vacant area is one of the areas that may be the boundary between water and land in coastal areas so that it can divide the two types of areas and depends on the moisture content of the area.

3.2 Support Vector Machine (SVM) Application

Based on the classification results using Support Vector Machine (SVM) with two classes, namely land (white) and water (black), we used 620 sample points, consisting of 310 points for water and 310 points for land, with a division of 70% training data and 30% validation data [31]. When training the SVM classifier, we chose the Radial Basis Function (RBF) kernel type and the cost parameter (C) = 10. The use of the RBF kernel is very effective because it has a good ability to handle non-linear data and distinguish two classes more optimally [19]. Choosing a cost value of 10, the SVM model used becomes more sensitive to

misclassification of the data used. Where the fines for misclassified data get really significant. Although the model becomes more sensitive to noise or minor data fluctuations, it is more exact in separating the two classes [19].

The classification outcomes from 2016 and 2023 exhibit variations in class distribution. In 2016, the classification results indicated that the water (black) class predominated in aquatic regions, including seas and rivers, whereas the land (white) class prevailed in most terrestrial areas (Figure 4). In 2023, it can be seen from the classification results that there is a little noise that occurs in the sea area, where many white spots represent the land class. The water class (black) also increasingly spreads in the land area in 2023 (Figure 4). These changes occur due to several possible factors, such as the influence of sedimentation, or the rise of water areas due to weather and human activities [32, 33]. Another factor is the image data, which may contain noise that escapes pre-processing or bias also caused by the recording of the Sentinel-1 product.

The class distributions in both years showed a good quality of separation between water and land, with sharp and consistent classification results. With a balanced number of samples between the two classes, 310 for water and 310 for land and a reasonable proportion of training and validation data, the SVM models trained tended to give accurate results.The map visualization shows that the SVM successfully utilizes the backscatter pattern of the radar data to distinguish between water and land classes.

The choice of an RBF kernel with an adequately elevated cost parameter facilitates optimal differentiation between the two classes, yielding a classification map with a distinct boundary separating water from land. The alterations noted between 2016 and 2023 signify that expansion transpired in 2023. The presence of noise in the Sentinel-1 image is shown by sea areas being classified as land (white), which is deemed a mistake. To assess the effectiveness of this SVM model, numerical assessments such as Overall Accuracy (OA) and Kappa Coefficient must be conducted to ascertain the model's predictive accuracy. The results facilitate further investigation to comprehend the origins of these changes, stemming from both natural processes and anthropogenic activity in the region.

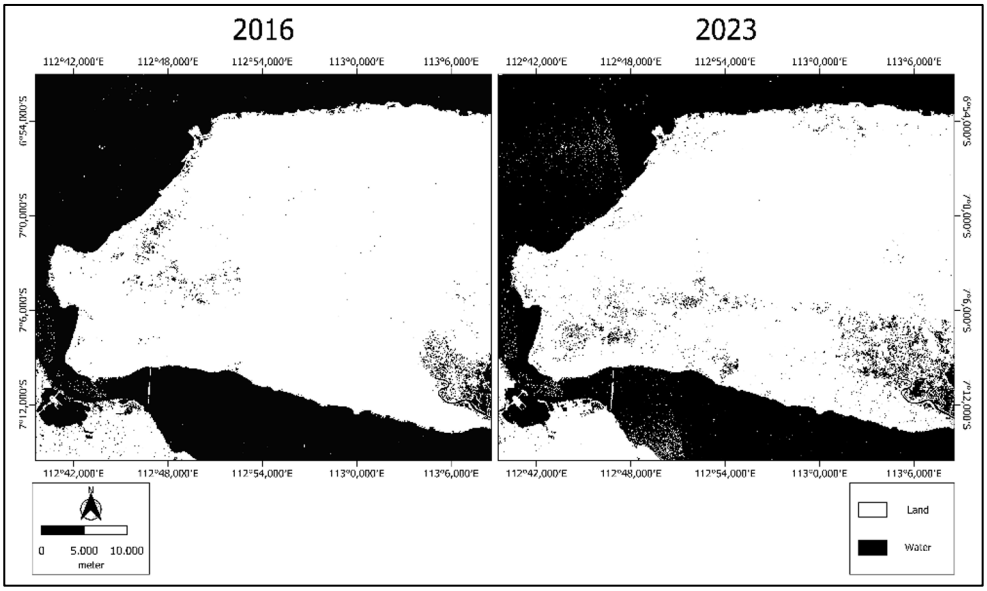

Figure 4. Segments of Shoreline 2013 and 2024

3.3 Accuracy of SVM Model

The assessment of the SVM model utilizing the Radial Basis Function (RBF) kernel employs two evaluation metrics: overall accuracy and the kappa coefficient. The overall accuracy results recorded in 2016 and 2023 are 99.5% and 99%, respectively. The Kappa Coefficient yielded results of 0.99018 for 2016 and 0.98138 for 2023. From both evaluation results, it can be said that it is very good even though there was a slight decrease in the 2023 values. This decrease can be attributed to the noise that occurs in 2023 where there are several land classes (white) in areas that should be marine areas. However, the model in this study is good because it gets the OA and Kappa Coefficient values which are included in the very good category and can separate the water and land areas to further extract the coastline from the classification results with the SVM model [16, 31]. Other studies have compared the accuracy of SVM with other machine learning, namely Random Forest (RF) and Convolutional Neural Network (CNN) but the highest value is produced by the RF method [47]. The RF accuracy value is 95%, the SVM accuracy value is 92% and the CNN method is 91% [46, 48]. The use of SVM on our data has a high accuracy value compared to these studies. Therefore, further research is needed to determine the performance of the three methods to apply the data used in this study, as well as for model exploration and data availability.

Table 2. Overall accuracy (OA) and kappa coefficient of Sentinel-1 image with SVM

Year	Satellite	Overall Accuracy (%)	Kappa Coefficient
2016	Sentinel-1	99.5	0.99018
2023	Sentinel-1	99	0.98138

3.4 Shoreline Extraction Result

The coastline extraction results obtained from classification with the SVM method show differences in 2016 and 2023. The coastline marked in red is the coastline in 2016, and green for 2023 (Figure 5). It can be seen from the results in Segment A that, visually, there are several areas where accretion and abrasion are balanced. In Segment B, there is a significant difference that occurs in the coastline in 2023, where the coastline enters the land area. This may occur due to the area being a pond area adjacent to the sea, so that it is identified as water and joins the sea area. In addition, there is visually balanced accretion and abrasion in the segment (Figure 5). In Segment C, there is one area of significant difference, where in 2023, there is an increase in the shoreline from 2016, as seen from the overlay of the two shorelines (Figure 5). Segment D has a few cases that are quite different because there are several beachfront buildings that are exposed to abrasion, so that they appear to recede. Besides that, the development of beachfront construction is also balanced in several areas of Segment D (Figure 5). Segment E looks balanced in the western part because, in some areas, there is the same abrasion and accretion. However, it is different from the eastern area, which is dominated by abrasion.

4 Conclusions

This study successfully showed the changes in the coastline in Bangkalan Regency using Sentinel-1 SAR data in 2016 and 2023. With the Support Vector Machine (SVM) method using the Radial Basis Function (RBF) kernel, the classification results show a sharp and accurate separation between water and land areas, with an overall accuracy of 99.5% (2016) and 99% (2023), and kappa coefficients of 0.99018 and 0.98138, respectively. The analysis showed significant differences in some shoreline segments, with varying indications of abrasion and accretion. Factors causing change include natural processes such as

sedimentation and human activities, including pond development and coastal construction. Although the model performed very well, some classification errors related to noise were still identified, especially in the 2023 data. This study confirms the potential of SAR data and SVM methods in monitoring shoreline dynamics, which can be further utilized for environmental analysis and coastal area management.

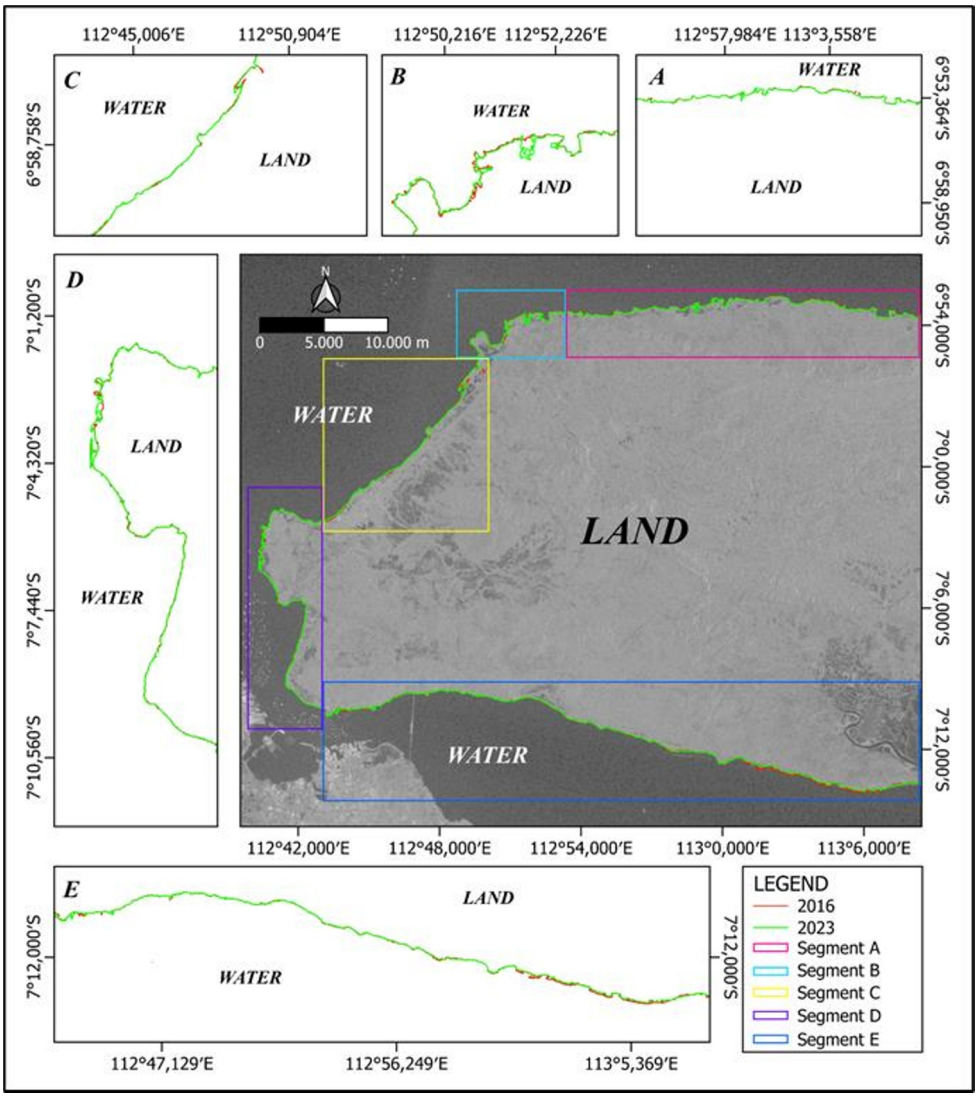

Figure 5. 2016 and 2023 shoreline extraction results after SVM classification

Acknowlegment

We would like to thank God Almighty for His mercy and grace so that we can complete this research. We would also like to thank the reviewers who provided useful suggestions to improve this paper. We would also like to thank the provider of Sentinel-1 European Space Agency for the open source data. Our gratitude also goes to the Department of Marine Science and the Oceanography Laboratory for University of Trunojoyo Madura for helping to equip facilities and infrastructure during the research.

As well as to all family, friends and all partner who have helped and supported in completing this research.

References

1. Abidin, Z., Setiawan, B., Muhaimin, A. W., & Shinta, A. (2021). The role of coastal biodiversity conservation on sustainability and environmental awareness in mangrove ecosystem of southern Malang, Indonesia. Biodiversitas Journal of Biological Diversity, 22(2).
2. Rizzetto, F. (2020). Effects of climate change on the morphological stability of the Mediterranean Coasts: Consequences for tourism. Climate Change, Hazards and Adaptation Options: Handling the Impacts of a Changing Climate, 761-775.
3. Melet, A., Teatini, P., Le Cozannet, G., Jamet, C., Conversi, A., Benveniste, J., & Almar, R. (2020). Earth observations for monitoring marine coastal hazards and their drivers. Surveys in Geophysics, 41, 1489-1534.
4. Pujianiki, N. N. (2022, December). Coastline changes monitoring induced by man-made structures using synthetic aperture radar: A new simple approach. In IOP Conference Series: Earth and Environmental Science (Vol. 1117, No. 1, p. 012041). IOP Publishing.
5. Dasari, K., Anjaneyulu, L., & Nadimikeri, J. (2022). Application of C-band Sentinel-1A SAR data as proxies for detecting oil spills of Chennai, East Coast of India. Marine Pollution Bulletin, 174, 113182.
6. Li, C., Chen, W., Wang, Y., Wang, Y., Ma, C., Li, Y., ... & Zhai, W. (2022). Mapping winter wheat with optical and SAR images based on Google Earth Engine in Henan Province, China. Remote Sensing, 14(2), 284.
7. Pramudya, F. S., Pan, J., Devlin, A. T., & Lin, H. (2021). Enhanced estimation of significant wave height with dual-polarization Sentinel-1 SAR imagery. Remote Sensing, 13(1), 124.
8. Soudani, K., Delpierre, N., Berveiller, D., Hmimina, G., Vincent, G., Morfin, A., & Dufrene, E. (2021). Potential of C-band Synthetic Aperture Radar Sentinel-1 time-series for the monitoring of phenological cycles in a deciduous forest. Int. J. Appl. Earth Obs. Geoinformation, 104, 102505
9. Li, X. M., Sun, Y., & Zhang, Q. (2020). Extraction of sea ice cover by Sentinel-1 SAR based on support vector machine with unsupervised generation of training data. IEEE Transactions on Geoscience and Remote Sensing, 59(4), 3040-3053.
10. Amitrano, D., Martino, G.D., Guida, R., Iervolino, P., Iodice, A., Papa, M.N., Riccio, D., & Ruello, G. (2021). Earth Environmental Monitoring Using Multi-Temporal Synthetic Aperture Radar: A Critical Review of Selected Applications. Remote. Sens., 13, 604.
11. Armono, H. D., Citrosiswoyo, W., & Muzaki, F. K. (2024). Shoreline change model after artificial reefs deployment in Tlangoh, Bangkalan, Madura. In BIO Web of Conferences (Vol. 89, p. 09002). EDP Sciences.
12. Panjaitan, J. P., & Maulana, F. (2024). Mapping shoreline changes using Landsat Imagery at Pemalang, Central Java Province, Indonesia. In BIO Web of Conferences (Vol. 106, p. 04011). EDP Sciences.
13. Widiawaty, M. A., Nandi, H. M., & Murtianto, H. (2020). Physical and social factors of shoreline change in Gebang, Cirebon Regency 1915–2019. Geospatial Information, 4(1), 327-334.

14. Dede, M., Susiati, H., Widiawaty, M. A., Kuok-Choy, L., Aiyub, K., & Asnawi, N. H. (2023). Multivariate analysis and modeling of shoreline changes using geospatial data. *Geocarto International*, *38*(1), 2159070.
15. Arum, Y. P. (2021, July). Analysis of shoreline changes using the bilko method on landsat imagery in Karawang regency (1999-2019). In Journal of Physics: Conference Series (Vol. 1943, No. 1, p. 012009). IOP Publishing.
16. Dike, E. C., Oyetunji, A. K., & Amaechi, C. V. (2023). Shoreline Delineation from Synthetic Aperture Radar (SAR) Imagery for High and Low Tidal States in Data-Deficient Niger Delta Region. Journal of Marine Science and Engineering, 11(8), 1528. https://doi.org/10.3390/jmse11081528
17. Mascolo, L., Lopez-Sanchez, J. M., & Cloude, S. R. (2021). Thermal noise removal from polarimetric Sentinel-1 data. IEEE Geoscience and Remote Sensing Letters, 19, 1-5.
18. Loukika, K. N., Keesara, V. R., & Sridhar, V. (2021). Analysis of Land Use and Land Cover Using Machine Learning Algorithms on Google Earth Engine for Munneru River Basin, India. Sustainability, 13(24), 13758. https://doi.org/10.3390/su132413758
19. Wale, P. B., Dhaigude, V., & Mishra, S. (2023). Comparative analysis of Image classification capabilities of Support Vector Machine (SVM) and Random Forest (RF) with Google Earth Engine (GEE) platform: A case study of Sangamner, Maharashtra. Intercontinental Geoinformation Days, 6, 113-116.
20. Masruroh, U. (2022). Konservasi dan Pemberdayaan "Peran CSR PHE WMO dalam Pemberdayaan Masyarakat Pesisir di Labuhan, Bangkalan". Eastasouth Journal of Effective Community Services, 1(02), 01-16.
21. Zhou, J., Gandomi, A. H., Chen, F., & Holzinger, A. (2021). Evaluating the quality of machine learning explanations: A survey on methods and metrics. Electronics, 10(5), 593.
22. Yang, Y., Yang, D., Wang, X., Zhang, Z., & Nawaz, Z. (2021). Testing Accuracy of Land Cover Classification Algorithms in the Qilian Mountains Based on GEE Cloud Platform. Remote Sensing, 13(24), 5064. https://doi.org/10.3390/rs13245064
23. Waleed, M., Mubeen, M., Ahmad, A., Habib-ur-Rahman, M., Amin, A., Farid, H. U., ... & El Sabagh, A. (2022). Evaluating the efficiency of coarser to finer resolution multispectral satellites in mapping paddy rice fields using GEE implementation. Scientific Reports, 12(1), 13210.
24. Sabery, S. M., Bystrov, A., Navarro-Cía, M., Gardner, P., & Gashinova, M. (2021). Study of Low Terahertz Radar Signal Backscattering for Surface Identification. Sensors, 21(9), 2954. https://doi.org/10.3390/s21092954
25. Zhang, B., Wdowinski, S., Gann, D., Hong, S. H., & Sah, J. (2022). Spatiotemporal variations of wetland backscatter: The role of water depth and vegetation characteristics in Sentinel-1 dual-polarization SAR observations. Remote Sensing of Environment, 270, 112864.
26. Hoffmeister, B. K., Gray, A. J., Sharp, P. C., Fairbanks, L. C., & Huang, J. (2020). Ultrasonic bone assessment using the backscatter amplitude decay constant. Ultrasound in Medicine & Biology, 46(9), 2412-2423.
27. Gomez, C., Su, R., De Groot, P., & Leach, R. (2020). Noise reduction in coherence scanning interferometry for surface topography measurement. Nanomanufacturing and Metrology, 3(1), 68-76.

28. Mullissa, A., Vollrath, A., Odongo-Braun, C., Slagter, B., Balling, J., Gou, Y., ... & Reiche, J. (2021). Sentinel-1 sar backscatter analysis ready data preparation in google earth engine. Remote Sensing, 13(10), 1954.
29. Zehner, M., Dubois, C., Thiel, C., Schellenberg, K., Rüetschi, M., Brenning, A., Baade, J., & Schmullius, C. (2023). Accounting for Deciduous Forest Structure and Viewing Geometry Effects Improves Sentinel-1 Time Series Image Consistency. IEEE Transactions on Geoscience and Remote Sensing, 61, 1-13.
30. Wang, Q., Lohse, J. P., Doulgeris, A. P., & Eltoft, T. (2023). Data augmentation for SAR sea ice and water classification based on per-class backscatter variation with incidence angle. IEEE Transactions on Geoscience and Remote Sensing, 61, 1-15.
31. Loukika, K. N., Keesara, V. R., & Sridhar, V. (2021). Analysis of Land Use and Land Cover Using Machine Learning Algorithms on Google Earth Engine for Munneru River Basin, India. Sustainability, 13(24), 13758. https://doi.org/10.3390/su132413758
32. Irham, M., Suri, R., Setiawan, I., & Fuadi, A. (2021, February). Spatial analysis of accretion, abrasion and shoreline change in banda aceh costal area. In IOP Conference Series: Earth and Environmental Science (Vol. 674, No. 1, p. 012046). IOP Publishing.
33. Owens, P. N. (2020). Soil erosion and sediment dynamics in the Anthropocene: a review of human impacts during a period of rapid global environmental change. Journal of Soils and Sediments, 20, 4115-4143.
34. Sebastianelli, A., Del Rosso, M. P., Ullo, S. L., & Gamba, P. (2022). A speckle filter for Sentinel-1 SAR ground range detected data based on residual convolutional neural networks. IEEE Journal of Selected Topics in Applied Earth Observations and Remote Sensing, 15, 5086-5101.
35. Sahithi, V. S., Iyyanki, M., & Giridhar, M. V. S. S. S. (2022). Analysing the sensitivity of SVM kernels on hyperspectral imagery for land use land cover classification. Journal of Image Processing and Artificial Intelligence, 8(2), 15-23.
36. Pani, A. K. (2022). Non-linear process monitoring using kernel principal component analysis: A review of the basic and modified techniques with industrial applications. Brazilian Journal of Chemical Engineering, 39(2), 327-344.
37. Razaque, A., Ben Haj Frej, M., Almi'ani, M., Alotaibi, M., & Alotaibi, B. (2021). Improved support vector machine enabled radial basis function and linear variants for remote sensing image classification. Sensors, 21(13), 4431.
38. Hong, Y., Xie, T., Luo, L., Wang, M., Li, D., Zhang, Q., & Xu, T. (2024). Area extraction and growth monitoring of sugarcane from multi-source remote sensing images under a polarimetric SAR data compensation based on buildings. *Geo-spatial Information Science*, 1-18.
39. Gierszewska, M., & Berezowski, T. (2022). On the role of polarimetric decomposition and speckle filtering methods for C-Band SAR wetland classification purposes. *IEEE Journal of Selected Topics in Applied Earth Observations and Remote Sensing*, *15*, 2845-2860.
40. Kumar, D. (2021). Urban objects detection from C-band synthetic aperture radar (SAR) satellite images through simulating filter properties. *Scientific Reports*, *11*(1), 6241.
41. Nesbit, P. R., Hubbard, S. M., & Hugenholtz, C. H. (2022). Direct georeferencing UAV-SfM in high-relief topography: Accuracy assessment and alternative ground control strategies along steep inaccessible rock slopes. *Remote Sensing*, 14(3), 490.

42. Ferreira, Z. A., & Cabral, P. (2022). A Comparative study about vertical accuracy of four freely available digital elevation models: a case study in the Balsas river watershed, Brazil. *ISPRS International Journal of Geo-Information*, 11(2), 106.
43. Tian, B., Zhang, F., Lang, F., Wang, C., Wang, C., Wang, S., & Li, J. (2022). A Novel Water Index Fusing SAR and Optical Imagery (SOWI). *Remote Sensing*, *14*(21), 5316.
44. Najem, S., Baghdadi, N., Bazzi, H., & Zribi, M. (2024). Incidence Angle Normalization of C-Band Radar Backscattering Coefficient over Agricultural Surfaces Using Dynamic Cosine Method. *Remote Sensing*, 16(20), 3838.
45. Frolking, S., Milliman, T., Mahtta, R., Paget, A., Long, D. G., & Seto, K. C. (2022). A global urban microwave backscatter time series data set for 1993–2020 using ERS, QuikSCAT, and ASCAT data. *Scientific Data*, *9*(1), 88.
46. Manomba-Mbadinga, N., Niculescu, S., Zaabar, N., Mombo, J. B., & Xie, G. (2023, October). Grand Libreville (Gabon) coastline using machine learning and convolutional neural network detection and automatic extraction of the methods. In *Earth Resources and Environmental Remote Sensing/GIS Applications XIV* (Vol. 12734, p. 1273402). SPIE.
47. Huo, W., Li, W., Zhang, Z., Sun, C., Zhou, F., & Gong, G. (2021). Performance prediction of proton-exchange membrane fuel cell based on convolutional neural network and random forest feature selection. *Energy Conversion and Management*, *243*, 114367.
48. Xie, G., & Niculescu, S. (2021). Mapping and monitoring of land cover/land use (LCLU) changes in the crozon peninsula (Brittany, France) from 2007 to 2018 by machine learning algorithms (support vector machine, random forest, and convolutional neural network) and by post-classification comparison (PCC). *Remote Sensing*, *13*(19), 3899.